



Theoretical and Experimental Investigation on Mechanical Behavior of Aluminum to Aluminum Tubular Bonded Lap Joint under Pure Torsion and a Finite Element Comparison with Hybrid Rivet/Bonded Joint

Mohiedin Yousefi¹, Saeed Rahnama², Mahmood Farhadi Nia³

¹ Ph.D. Candidate, Department of Mechanical Engineering, University of Birjand, Birjand, Iran, Email: myousefi@birjand.ac.ir

² Assistant Professor, Department of Mechanical Engineering, University of Birjand, Birjand, Iran, Email: srahnama@birjand.ac.ir

³ Assistant Professor, Department of Material Engineering, Malek Ashtar University of Technology, Tehran, Iran, Email: mahmood_farhadinia@mut.ac.ir

Received December 30 2019; Revised March 05 2020; Accepted for publication March 16 2020.

Corresponding author: S. Rahnama (srahnama@birjand.ac.ir)

© 2022 Published by Shahid Chamran University of Ahvaz

Abstract. The combination of mechanical and bonded joints creates a new connection type, called hybrid joint which has the benefits of both mechanical and bonded joints. In this research, the mechanical behavior of the tubular bonded lap joint between aluminum tubes subjected to pure torsion has been investigated experimentally and numerically, and the results have been compared. The mechanical behavior of the hybrid (rivet/bonded) joint has been investigated numerically and the outcomes have been compared. The adhesive and rivets have cohesive elements and bushing connector elements, respectively. The results from the hybrid joints and the damage mechanism show that the rivets change the interface shear stress and the stress distribution of the joint, and affect the joint's torque capacity and strengths. It has been observed that for specimens with overlap lengths close to effective length, the hybrid joint is more effective.

Keywords: Hybrid Joint, Finite Element Method, Bushing Connector Element, Cohesive Element.

1. Introduction

Tube structures become more popular in structural applications such as transmission shafts, robot arms, crash boxes, space frames, side door impact beams, and construction industry[1]. Several types of research on tubular lap joints have been done under pure torsion [2]. Since the connection method between parts plays an important role in the assembly of the structures, studying the properties and behavior of the connection area is important [3]. In some cases, instead of mechanical joints, adhesively bonded joints have better influence because of, better stress distribution and fatigue performance, and even joint dissimilar adherends together, and the load between two adherends transferred by the adhesive layer. Some of the investigations were done on the stress behavior of the tubular joints subjected to pure torsion with theoretical and the finite element (FE) approaches. The combination of mechanical and adhesive joints creates a new connection type called hybrid joints [4]. Because of hybrid joint's higher abilities compared to mechanical and bonded joints, such as higher strength, better fatigue lifetime, and load capacity, these types of joints have been used in several engineering structures [5]. Also, the stress concentration around the fastener position is reduced by adhesive while the fastener decreases the relative displacement of the bonded area.

Adams and Peppiatt have analyzed the stress of adhesive bonded tubular lap joint, with adding the thickness of adhesive to their theory [6]. Chen and Cheng analyzed the stress distribution in adhesive bonded tubular lap joint subjected to torsion. Their analysis was based on elasticity theory with variational principle of complementary energy. Special attention had been given to the high-stress intensities in the end zones of the joint, and a stress concentration factor was deduced [7]. Reedy, et. al, have investigated strength and fatigue resistance of composite to metal tubular lap joints. They measured the axial strength and fatigue resistance of adhesively tubular lap joints in thick-walled E-glass epoxy composite to aluminum (Al), by tensile and compressive loading [8]. Hosseinzadeh, et. al, have reported an engineering approach analysis for design metallic pipe joints under torsion by the finite element method (FEM) [9, 10]. Das and Pradhan have investigated adhesive failure analyses of bonded tubular single lap joints in laminated fiber-reinforced plastic composites [11]. All of the previous reports didn't include the cohesive behavior of the adhesive in the bonded area. Ouyang and Li were worked on a cohesive zone model (CZM), based on analytical solutions for adhesively bonded pipe joints under torsion, which include the cohesive stiffness as a parameter in the calculation of interface shear stress [12].



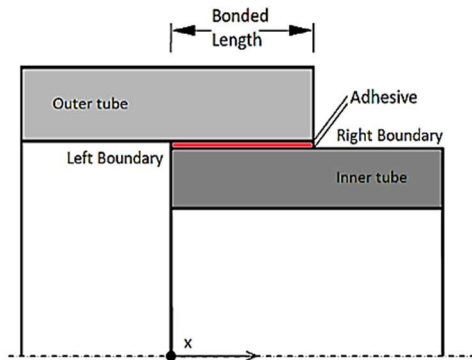


Fig. 1. The structure of the tubular bonded lap joint.

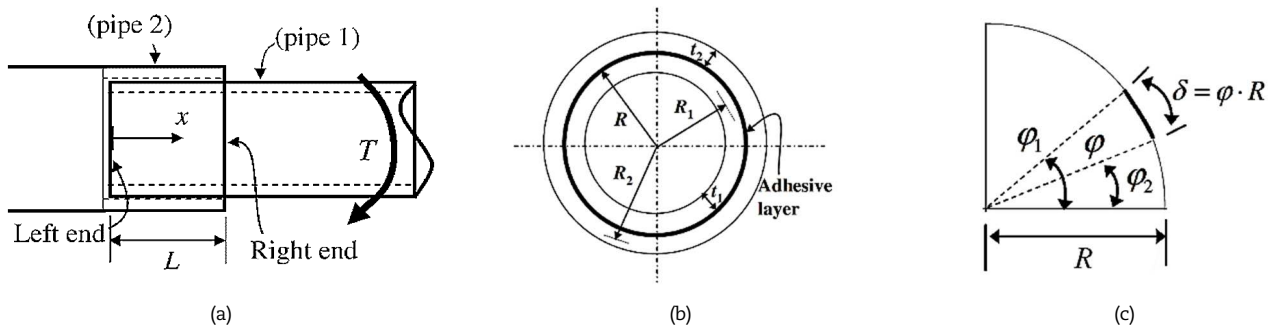


Fig. 2. Tubular bonded lap joint and define parameters (a) side view of the joint, (b) cross-section view of the joint, (c) relative rotation and circumferential relative displacement [12].

According to Fig. 1, a tubular lap joint has been created by using an adhesive between two surfaces of the substrates with a certain bonded length. Under pure torsion, there will be no bending effects at the bonded area in the tubular lap joint [9, 10, 12]. By increasing the adhesive thickness in the bonded line, the maximum shear stress at the ends of the bonded area decreases [13]. Effective length for overlap area affected shear stress behavior [12, 13]. The shear modulus and polar moment of inertia of substrates were caused specific efficacy on the failure initiation under pure torsion [12, 14]. For layered composite tubes such as E-glass tubes, the maximum stress at the ends of the lap joints depends on the orientation of layups. The [0/90] layup has higher shear stress than [-45/45] layup under pure torsion [14].

In this research mechanical behavior of tubular bonded lap joint between Al to Al tubes under pure torsion has been investigated numerically and experimentally. The numerical approach has been done with ABAQUS CAE finite element analysis software package. The experimental analysis has been done on specific Al to Al specimen with a torsion test machine. The torque-angle diagram and the torque capacity for specimen have been recorded. The results from the FE and experimental analyses compared and reported. The tubular hybrid (rivet/bonded) lap joint subjected to pure torsion has been studied with bushing elements connectors (fastener method) for the first time. The comparison of results between the bonded and hybrid joints shows some interesting differences.

2. Theory of Tubular Joint

Based on Ouyang's research in [12] and Fig. 2a, b, and c., which described the geometries and parameters, it has been assumed that the torque carried only by the adherends. By use of the equivalent linear elastic cohesive law, it has been reported by Ouyang in [12] and Hossainzade in [9, 10] that, interface shear stress reach fracture value under mode III and the k_e of the linear elastic cohesive law calculated in eq. (1).

$$k_e = \frac{G_a}{h_a} \tag{1}$$

The $\varphi(x)$ at any location in the bonded area calculated from eq. (2) [12]

$$\varphi(x) = T \left[\frac{1}{\alpha G_1 J_1} + \frac{1}{\alpha G_2 J_2} \exp(\alpha L) \right] \cdot \exp(-\alpha x) + T \left[\frac{1}{\alpha G_1 J_1} + \frac{1}{\alpha G_2 J_2} \exp(-\alpha L) \right] \cdot \exp(\alpha x) \tag{2}$$

$$\alpha = \sqrt{2\pi R^3 \cdot k_e \frac{G_1 J_1 + G_2 J_2}{G_1 J_1 \cdot G_2 J_2}}$$

The amount of l_e has been measure by eq. (3)[12].

$$l_e = \frac{1}{\alpha} \cdot \ln \left[\frac{0.99\mu + \sqrt{(0.99\mu)^2 + 1 - 0.99^2}}{1 - 0.99} \right] \tag{3}$$



$$\mu = \frac{G_1 J_1}{G_2 J_2} \text{ when } G_1 J_1 < G_2 J_2$$

$$\mu = \frac{G_2 J_2}{G_1 J_1} \text{ when } G_1 J_1 > G_2 J_2$$

The interface shear stress distribution was extracted from eq. (4).

$$\tau(x) = \frac{\varphi(x) R G_a}{h_a} \quad (4)$$

Swift's analytical method in [15, 16] represented that, the fasteners equivalent stiffness in hybrid joints have been used, to apply the stiffness of the connector in the finite element model. By using bushing elements in the simulation, the stiffness values add from eq. (5).

$$K_1 = \frac{E_1 D}{[A + C \left(\frac{D}{t_1} + \frac{D}{t_2} \right)]}$$

$$K_2 = \frac{E_2 D}{[A + C \left(\frac{D}{t_1} + \frac{D}{t_2} \right)]} \quad (5)$$

$$K_3 = \frac{E_f D^2 \pi}{[2(t_1 + t_2)]}$$

K_1 , and K_2 are the stiffness of the fastener in contact with the adherends and K_3 is the stiffness of the fastener.

3. Experimental Analysis

The experimental section includes the investigation of the tensile properties of Ghaffari chemical industrial Co. Super Special (S.S) adhesive (Fig. 3a.). Additionally, adhesively bonded tubular lap joint specimens between Al to Al with S.S adhesive manufactured and the torsional test has been done.

According to the S.S's datasheet in [17] and ASTM D638-03, the tensile test has been done. With the same volume fraction ratio for resin and hardener of the S.S, the silicone mold filling up with combined raw adhesive. By the use of Veeco V300 high vacuum chamber with 0.2mbar as the pressure of the chamber, in about 3 hours the bubbles and voids disappeared with the degassing process in specimens (see Fig. 3b, c, and d). The mold with raw dog bone specimens cures and post-cured up to 40°C for about 16 hours. The finalized specimens were checked by an optical microscope to analyses the distribution of bubbles and voids (Fig. 3e.). The tensile test has been done with Zwick Z250 tensile test machine at the speed of 5mm/min and by the use of extensometer to measures the test specimen's elongation to characterize strain (Fig. 4a.). The average results of the tensile tests for 3 specimens were shown in Fig. 4b and the elastic modulus was found about 2100 MPa. The broken dog bone specimen shows in Fig. 4c.

The tubular adhesively bonded lap joint specimen between Al to Al is shown in Fig. 5a. The Al tubes were made from Al 7075-T6. All of the tubes washed by liquid soap and cleaned in the ultrasonic washing machine and cleaned with deionized water before used to bond together with S.S adhesive. The geometry of specimens and explosive views were shown in Fig. 5b&c., respectively. The specimen has a 10mm overlap bonded length and 0.2mm adhesive thickness. The steel (St 1035) core provides the 0.2mm adhesive thickness and centering the tubes. To assemble the tubes the inner and outer surfaces in the bonded area have been stained with adhesive and the inner tube has been placed in to engage with the outer tube at the bonded location. The pushed out and remain adhesives have been removed to minimize the effect of adhesive fillets at the boundaries. The prepared specimens with raw adhesive cure and post-cure at 40°C for 16 hours. The steel core has been removed after without any issues and the specimens with the use of manufactured fixture mounted on the torsional test machine to apply the torsion to the bonded region.

The torsional test has been done with the BST200 torsional device of Barsanj Electric Co., at the speed of 2 rpm until the bonded area breaks. The 3D model of specimen and manufactured fixture which mounts on the torsion machine has been shown in Fig. 6b. The average result of the three torsional tests for Al to Al specimen as the torsion-angle diagram has been obtained. The torsion-angle diagram shows that the maximum torque value to failure was 170.05Nm. The brittle behavior of the S.S adhesive provides a sudden fracture with a small relative rotational angle between tubes.

4. Numerical Analysis

The ABAQUS CAE has been used as an industrial finite element software package to simulate the tubular adhesively bonded and hybrid lap joints. The S.S as adhesive, the Al 7075-T6 as tubes, and Al 5052 as rivet connectors have been used, respectively. The mechanical properties of these materials have been mentioned in Table.1.

Mesh sensitivity and validation results are performed based on the analytical solution and specimens' geometries from Ouyang's work in [12] for steel to steel pipe with IPCO adhesive. The steel adherends and IPCO adhesive have been assumed as isotropic elastic material with C3D8R elements. According to the obtained interface shear stress from the finite element method (FEM) and analytical analysis, the finite element result shows that the optimized mesh size for adhesive in the bonded region is 0.2mm. This mesh size achieved less than a 7% error between the finite element and analytical results with suitable simulation time.

The experimental analysis result between Al to Al tubular lap joint with S.S adhesive has been simulated with the finite element method and the torque-angle diagram has been extracted. The Al tubes assumed to be isotropic with C3D8R elements and the S.S adhesive effect has been simulated with COH3D8 cohesive elements. The elastic properties and traction separation behavior of S.S reported in Table.2. The finite element model and the boundary condition have been shown in Fig. 7a&b., respectively. The inner tube has been rotated with 2rpm and the results (torque-angle diagram) from both numerical and experimental approaches have been recorded in Fig. 8a. It has been observed that the experimental and FEM torque values at peak point have 170.05N.m and 167.14N.m, respectively. Also, the rotational angle degree at peak point recorded 0.31 and 0.33 degrees for experimental and numerical approaches, respectively.



Table 1. Mechanical properties of used materials.

Material	Tensile Modulus (MPa)	Poisson ratio
S.S. Ghaffari	2100	0.4 ^a
Al 7075-T6	72000	0.33
Al 5052	70000	0.33

^a Gaffari Co. data sheet [17]

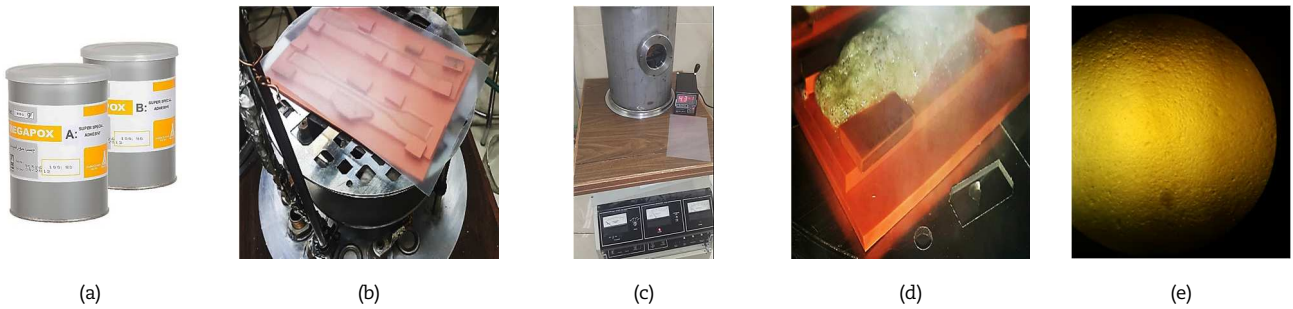


Fig. 3. (a) S.S adhesive, (b) filled up Silicone mold, (c) Veeco V300 high vacuum system, (d) degassing during the vacuum process, and (e) optical microscopic picture of specimen

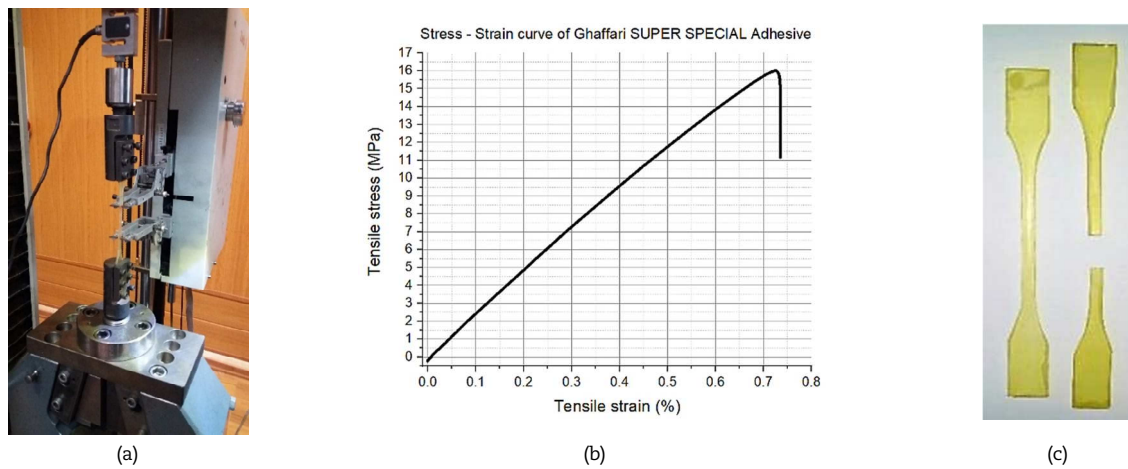


Fig. 4. (a) Zwick Z250 tensile test machine with extensometer and mounted specimen, (b) Stress-Strain curve of S.S adhesive, and (c) Dog bone specimen before and after the tensile test

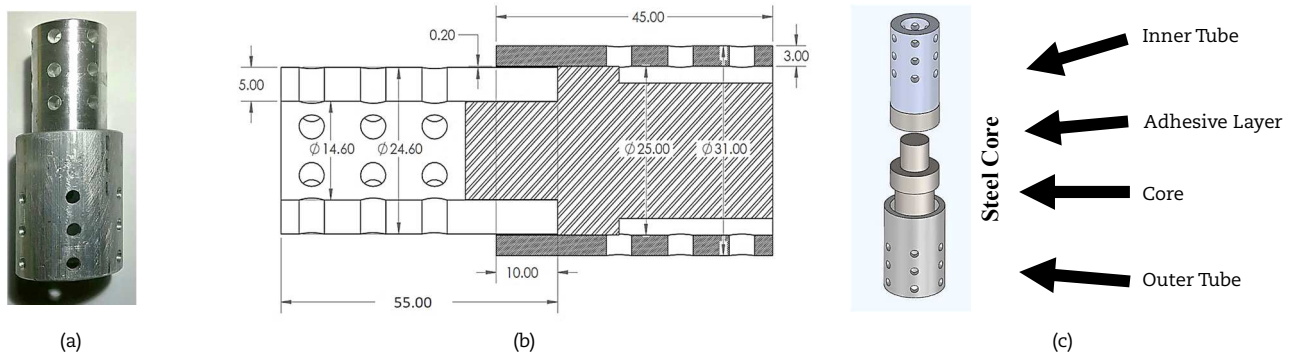


Fig. 5. (a) Al to Al adhesively bonded joint, (b) Geometry of specimen, and (c) explosive view and assemble method of specimens

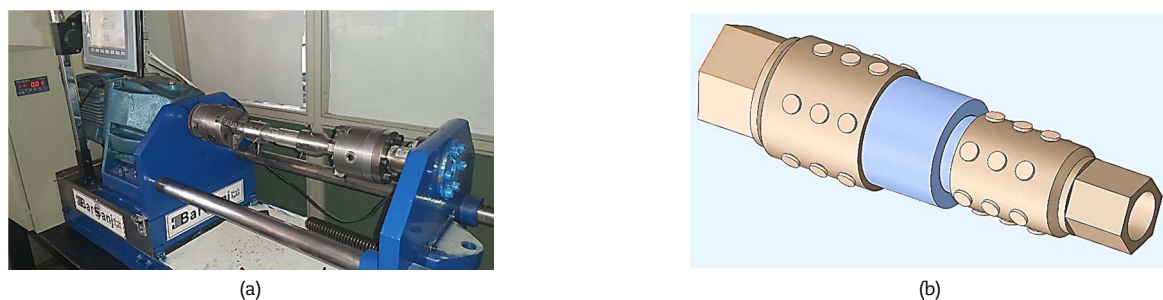


Fig. 6. (a) Barsanj Electric Co. BST300 torsion test machine, (b) 3D model of fixture and specimen



Table 2. Cohesive zone material parameters

Property	Value
Young's Modulus	2100 MPa
Shear's Modulus	699 MPa
Tensile Failure's Strength	28.9 MPa
Shear Failure's Strength	17.8 MPa
Toughness- G_f	0.9 N/mm

Table 3. Geometry in numerical analysis for Al to Al specimens.

Classification	1	2	3	4
Outer pipe length (mm)	55	45	55	45
Adhesive bonded length (mm)	20	10	20	10
Outer pipe thickness (mm)	5	5	3	3
Inner pipe average radius (mm)	9.8	9.8	9.8	9.8
Outer pipe average radius (mm)	15	15	14	14

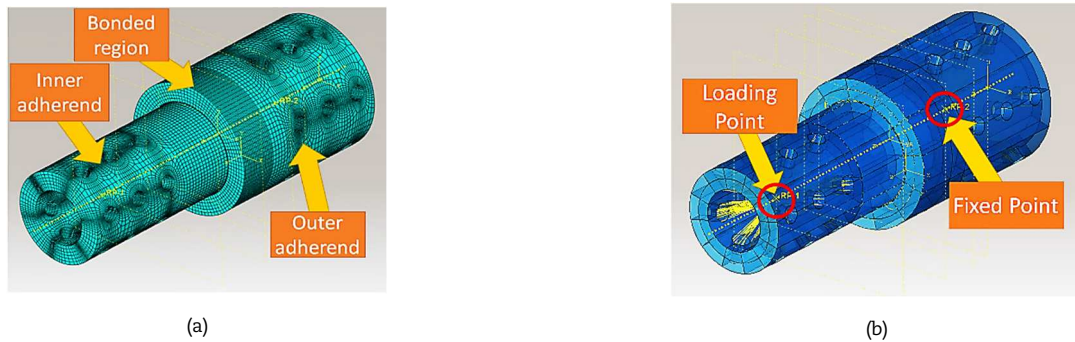


Fig. 7. (a) Finite element model, and (b) boundary condition for Al to Al tubular specimen with 10mm overlap length and 0.2mm S.S adhesive thickness

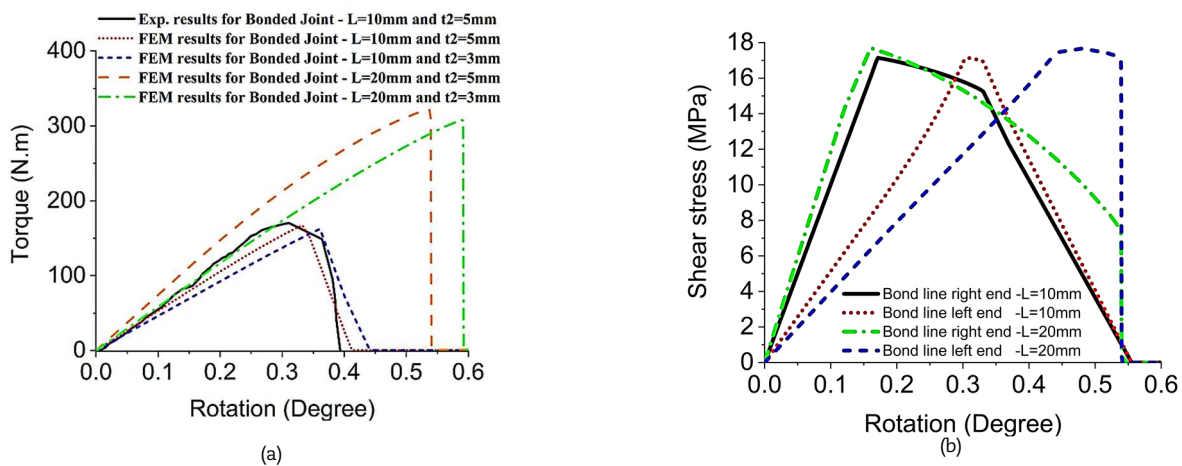


Fig. 8. (a) Torque-angle diagram for Al to Al adhesively bonded tubular lap joint specimens, and (b) shear stress-angle diagram for specimens with 10mm and 20mm overlap length with 5mm tubes thickness

The shear stress values for boundary elements of S.S adhesive has been extracted and recorded in Fig. 8b. For the 10mm overlap length. It observed that the stress for the right end (see Fig. 2a.) reaches the failure point faster than the left end. It means that, same as Ouyang reports in [11], the relation between GJ values for each pipe identifies the maximum stress location and the initiation of the adhesive fracture at the bond line. Furthermore, at the 0.33 degrees, the joint completely broke and the stress of boundary elements will have a value of zero. It should be noticed that at the 0.15 degrees the right boundary elements are in damage zone and their stress value is decreasing until reach the 0.33 degrees while the left boundary elements are still increasing their stress's value up to peak point.

The finite element model of Al to Al tubular lap joint with 10mm overlap length and 5mm tube's thickness has been analysis under 170N.m torsional load. The circumferential shear stress vs rotation angle of the S.S adhesive has been recorded and reported in Fig. 9a. It has been observed that under 170N.m applied torque, the adhesive reaches its final strength value.

The numerical analysis has been extended to other geometries which reported in Table.3. These specimens have been classified by their overlap length and outer tube thickness. In these specimens, the adhesive thickness fixed to 0.2mm. For the inner tube, the thickness, the length and the average radius have been assigned equal to 5mm, 55mm, and 9.8mm, respectively. It means that for all specimens, the inner tube parameters and adhesive thickness are fixed, and the change of overlap length and outer tube thickness have been investigated.

The torque-angle diagram for these classifications has been reported in Fig. 8a. It has been observed that the specimens with lower outer tube thickness due to the change in the stiffness of the specimen, have a higher angle at peak point while the maximum torque is lower than the specimens with higher outer tube thickness. Furthermore, the specimens with the 20mm overlap length have higher maximum torque up to peak point than specimens with the 10mm overlap because the higher overlap length increases the torque capacity of the joint. Additionally, the whole adhesive layer in 10mm overlap specimens has been affected by torsional load while for 20mm overlap length the middle part of adhesive has not been affected.



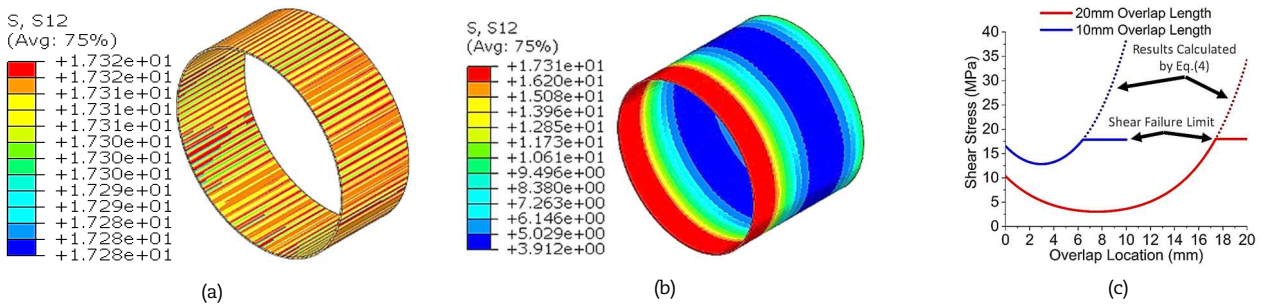


Fig. 9. The adhesive shear stress distributions subjected to 170N.m (a) FE results-10mm overlap length, (b) FE results-20mm overlap length and, (c) Analytical method results based on eq. (4).

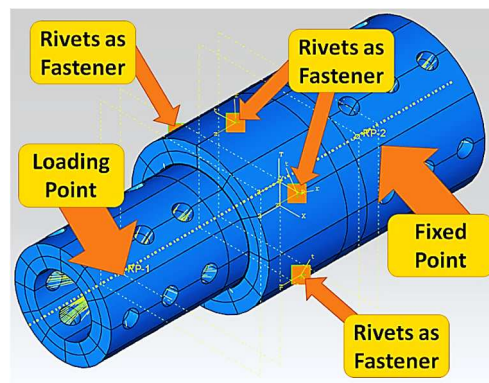
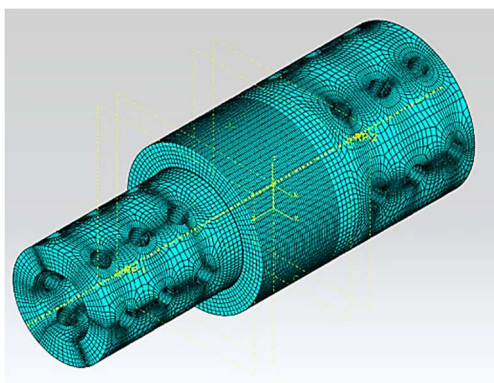
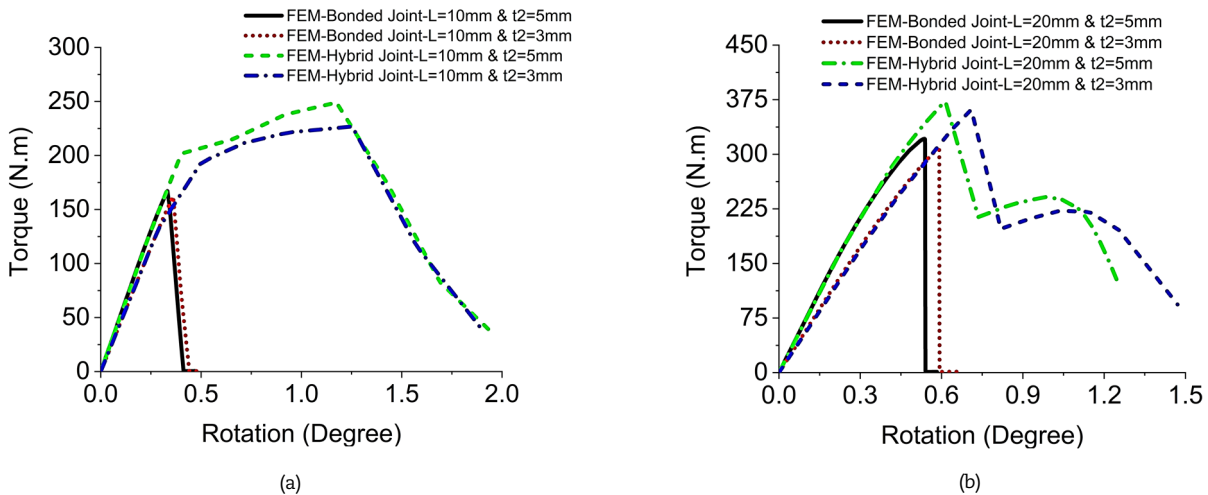


Fig. 10. (a) torque-angle diagram for 10mm overlap length hybrid specimens, (b) torque-angle diagram for 20mm overlap length hybrid specimens, (c) finite element model of hybrid joint with 20mm overlap length, and (d) boundary conditions and fastener locations of hybrid joint with 20mm overlap length

The shear stress for boundary elements of the two first classifications (see Table.3) has been recorded in Fig. 8b. It has been observed that for the 20mm overlap length, the right end boundary elements resist more than the 10mm overlap length up to the falling point. Additionally, the left end of the specimen with the 20mm overlap length reaches peak point at 0.45 degrees while in the specimen with the 10mm overlap length it is 0.3 degrees. Furthermore, from Fig. 8. It has been concluded that the falling part of diagrams for the specimen with 20mm overlap length is sudden while this behavior has not been observed in the 10mm overlap length. Because the whole adhesive layer in the specimen with 10mm overlap length affected by torsion, while in 20mm overlap specimens it is vice versa (see Fig. 9). This stress analysis expression has been observed with the analytical approach of Ouyang's research in [12].

By investigation on the shear stress results in the bonded area by finite element method (See Fig. 9a and b) and analytical method (See Fig. 9c), the outcomes have been obtained as below. The results from eq.4, which depend on the geometry and properties of the joint components, show that the shear stress in some positions passes the shear failure limit in the diagram (see Fig. 9c) when the specimens subjected to pure torque equal to 170N.m. Additionally, when the cohesive elements reach the failure limit and reach the fracture point, disappear and the overlap length changes during the torsional process which didn't consider in the eq.4. The experimental test and finite element with cohesive elements results for the specimen with the 10mm overlap length, which is lower than the effective length, show that the adhesive layer completely break under 170N.m but, the eq.4 doesn't show this phenomenon. The reasons for this contradiction are mentioned above. On the other hand for the specimen with the 20mm overlap length, which is higher than the effective length, the joint stays safe and the eq.4 shows a good similarity with finite element results. So, the eq.4 has a good complimentary outcome for overlaps higher than the effective length.



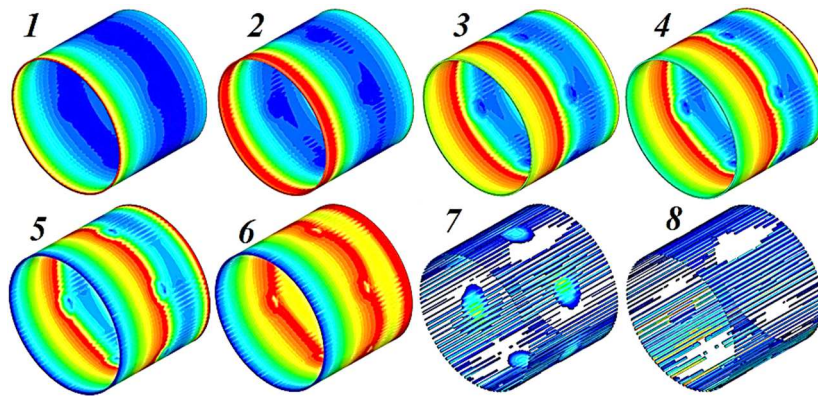


Fig. 11. The shear stress distribution of the adhesive layer and fasteners effect in sequence from 1 to 8 for 20mm overlap length and 5mm tube's thickness.

The torsional stiffness analysis from the torque-angle diagram shows that the stiffness is lower in specimens with smaller outer tube thickness while the rotational angle is higher. Furthermore, the specimens with higher overlap length have higher stiffness in the bonded joint. The comparison between experimental and FE results show an average of 8% error between them. The error starts to increase when the torsion-angle diagram reaches the peak point. The environment effects and adhesion properties between adhesive and adherends in experimental analysis affect the outcomes while in the FE analysis the properties of the components are independent of these impacts.

In the following, all of the classification specimens in Table.3 have been upgraded to hybrid (rivet/bonded) joints. Six Al 5052 rivets have been attached to the middle of the overlap length with the same angles to each other. The rivets have been defined with bushing element connectors, and elastic and damage properties. The properties of bushing elements have been calculated with eq.5 and assigned from Table.1 with the use of the fastener method in ABAQUS CAE. The same analysis from adhesively bonded joints has been replied for hybrid specimens and the results for 10mm and 20mm overlap lengths have been recorded in Fig. 10a and b, respectively. The finite element model and the 3D model of fasteners position in the hybrid joint specimen with 20mm overlap length and 5mm tubes thickness have been shown in Fig. 10c and d, respectively.

The results for the 10mm overlap show that the rivets increase the maximum torque for 5mm and 3mm outer tube thickness 44.2% and 34.7%, respectively. The results for the 20mm overlap show that the rivets increase the maximum torque for 5mm and 3mm outer tube thickness 16.9% and 17.5%, respectively. The comparison between overlap lengths shows that for the 10mm overlap, the failure of the joint is a combination of adhesive and rivet failure while for 20mm overlap length, the failure of the joint starts with the fracture of the adhesive and then the rivets' failure happens. The shear stress distribution of the adhesive layer with the 20mm overlap and 5mm tube thickness under the fastener effect has been recorded in Fig. 11 in sequence on with 8 steps of simulation.

5. Conclusion

In this research, the experimental and numerical analysis was carried out on the adhesively bonded and hybrid (rivet/bonded) joints between aluminum tubes subject to pure torsion. Cohesive elements (COH3D8) and bushing elements (fastener method) were used to investigate the adhesive and rivets effect, respectively. By the use of cohesive zone method and traction-separation properties of the adhesive and swift method for rivets as damageable connectors, the finite element analysis has been done on hybrid rivet/bonded joints. The damage mechanism from the numerical analysis shows that for bonded and hybrid joints, the ratio between GJ values of each tube indicates the damage initiation and propagation path of the bonded area. In the hybrid joint, damage initiation and propagation mechanism affected by the rivets which increases the torque capacity of the joint. The results show that for 10mm overlap length, which is close to the effective length, converting the adhesively bonded joint to the hybrid rivet/bonded joint increases the maximum torque capacity more than 30%. On the other hand, in hybrid rivet/bonded joints with 20mm overlap length, the rivets increase the torque capacity of the joint about 17% compared to adhesively bonded joints with the same overlap length.

Author Contributions

M. Yousefi conducted the experiments, analyzed the results, developed the numerical modeling and examined the validation. The manuscript was written through the contribution of all authors. All authors planned the scheme, initiated the project and suggested the experiments; discussed the results, reviewed and approved the final version of the manuscript.

Acknowledgments

The authors thank the Barsanj Electric Co. for the torsion machine and the University of Malek Ashtar for the laboratory equipment. The great gratitude for Prof. Filippo Berto and Prof. Andreas Echtermeyer at Norwegian University of Science and Technology and Prof. Norbert Enzinger at the Graz University of Technology for their scientific guidance.

Conflict of Interest

The authors declared no potential conflicts of interest with respect to the research, authorship, and publication of this article.

Funding

The authors received no financial support for the research, authorship, and publication of this article.



Data Availability Statements

The datasets generated and/or analyzed during the current study are available from the corresponding author on reasonable request.

Nomenclature

A	Constant values	L	Overlap joint length
C	Constant values	l_e	Effective length
D	Diameter of the fastener	R_1	Average radius of inner pipe
E_1	Young modulus of adherend 1	R_2	Average radius of outer pipe
E_2	Young modulus of adherend 2	R	Average radius of adhesive
E_f	Tensile modulus of fastener	T	Applied torque
G_a	Shear modulus of adhesive	t_1	Thicknesses of inner tube
G_1	Shear modulus of the inner tube	t_2	Thicknesses of outer tube
G_2	Shear modulus of the outer tube	δ	Circumferential relative displacement
h_a	Adhesive thickness	φ	Circumferential relative angle
J_1	Inner tube Polar moment of inertia	φ_1	Rotation of inner pipe
J_2	Outer tube Polar moment of inertia	φ_2	Rotation of outer pipe
k_e	Interface stiffness	τ	Interfacial shear stress
K_1, K_2, K_3	Stiffness values		

References

- [1] Sevkat, E., Tumer, H., Kelestemur, M.H., Dogan, S., Effect of torsional strain-rate and lay-up sequences on the performance of hybrid composite shafts, *Materials & Design*, 60, 2014, 310-9.
- [2] Shishesaz, M., Tehrani, S., The effects of circumferential voids or debonds on stress distribution in tubular adhesive joints under torsion, *The Journal of Adhesion*, 2019, 1-35.
- [3] Aimmanee, S., Hongpimolmas, P., Stress analysis of adhesive-bonded tubular-coupler joints with optimum variable-stiffness composite adherend under torsion, *Composite Structures*, 164, 2017, 76-89.
- [4] Esmaeili, F., Zehsaz, M., Chakherlou, T., Barzegar, S., Fatigue life estimation of double lap simple bolted and hybrid (bolted/bonded) joints using several multiaxial fatigue criteria, *Materials & Design*, 67, 2015, 583-95.
- [5] Gómez, S., Onoro, J., Pecharrroman, J., A simple mechanical model of a structural hybrid adhesive/riveted single lap joint, *International journal of Adhesion and Adhesives*, 27, 2007, 263-7.
- [6] Adams, R., Peppiatt, N., Stress analysis of adhesive bonded tubular lap joints, *The Journal of Adhesion*, 9, 1977, 1-18.
- [7] Chen, D., Cheng, S., Torsional stress in tubular lap joints, *International Journal of Solids and Structures*, 29, 1992, 845-53.
- [8] Reedy, E., Guess, T.R., Composite-to-metal tubular lap joints: strength and fatigue resistance, *International Journal of Fracture*, 63, 1993, 351-67.
- [9] Hosseinzadeh, R., Cheraghi, N., Taheri, F., An engineering approach for design and analysis of metallic pipe joints under torsion by the finite element method, *The Journal of Strain Analysis for Engineering Design*, 41, 2006, 443-52.
- [10] Hosseinzadeh, R., Taheri, F., Non-linear investigation of overlap length effect on torsional capacity of tubular adhesively bonded joints, *Composite Structures*, 91, 2009, 186-95.
- [11] Das, R., Pradhan, B., Adhesion failure analyses of bonded tubular single lap joints in laminated fibre reinforced plastic composites, *International Journal of Adhesion and Adhesives*, 30, 2010, 425-38.
- [12] Ouyang, Z., Li, G., Cohesive zone model based analytical solutions for adhesively bonded pipe joints under torsional loading, *International Journal of Solids and Structures*, 46, 2009, 1205-17.
- [13] Hipol, P.J., Analysis and optimization of a tubular lap joint subjected to torsion, *Journal of Composite Materials*, 18, 1984, 298-311.
- [14] Chon, C.T., Analysis of tubular lap joint in torsion, *Journal of Composite Materials*, 16, 1982, 268-84.
- [15] Doubrava, R., Effect of mechanical properties of fasteners on stress state and fatigue behaviour of aircraft structures as determined by damage tolerance analyses, *Procedia Engineering*, 101, 2015, 135-42.
- [16] Skorupa, A., Skorupa, M., Riveted lap joints in aircraft fuselage: design, analysis and properties, *Springer Science & Business Media*, 2012.
- [17] Thechnical datasheet of SUPER SPECIAL adhesive, Gaffari Chemical Industrial Co., 2005.

ORCID iD

Mohiedin Yousefi  <https://orcid.org/0000-0002-8208-6316>

Saeed Rahnama  <https://orcid.org/0000-0002-0256-047X>

Mahmood Farhadi Nia  <https://orcid.org/0000-0002-3105-1754>



© 2022 Shahid Chamran University of Ahvaz, Ahvaz, Iran. This article is an open access article distributed under the terms and conditions of the Creative Commons Attribution-NonCommercial 4.0 International (CC BY-NC 4.0 license) (<http://creativecommons.org/licenses/by-nc/4.0/>).

How to cite this article: Yousefi M., Rahnama S., Farhadi Nia M. Theoretical and Experimental Investigation on Mechanical Behavior of Aluminum to Aluminum Tubular Bonded Lap Joint under Pure Torsion and a Finite Element Comparison with Hybrid Rivet/Bonded Joint, *J. Appl. Comput. Mech.*, 8(2), 2022, 485-492. <https://doi.org/10.22055/JACM.2020.32081.1967>

Publisher's Note Shahid Chamran University of Ahvaz remains neutral with regard to jurisdictional claims in published maps and institutional affiliations.

